Supporting Information

Szell et al. 10.1073/pnas.1004008107

SI Text

This supplement to the paper "Multirelational organization of large-scale social networks in an online world" contains detailed information on the various network types analyzed, an overview of the game, notations of measures used, a detailed analysis of signed triad dynamics, and the null model and STC model for the social balance part.

Different Types of Social Interactions.

- *Friendship and enmity networks.* Players can anonymously mark others as friends or enemies, for any reason. The marked players are added to the marker's personal friends or enemies list. Additionally, every player has a personal "friend of" and "enemy of" list, displaying all players who have marked them as friend or enemy, respectively. Friend and enemy markings can be removed anytime.
- *Communication networks.* Private messages (PMs) are the prevalent form of communication within the game. It is similar to e-mail—a PM is only seen by sender and receiver.
- *Trade networks.* These are extracted by considering two kinds of trade possibilities between players: Either players meet and exchange game money and/or commodities, or players visit commercial outlets of other players and buy/sell commodities or equipment.
- *Attack networks.* For extracting attack networks, we select all attacks carried out by players on other players or on commercial outlets.
- *Bounty networks.* Links in bounty networks represent bounties, which are amounts of game money placed on other players or on their commercial outlets. Any player can collect a bounty by terminating the bountied player or destroying his commercial outlet.

How Players Get to Interact with Each Other. For a basic understanding of how the implementation of the game may shape the patterns of interactions between players, we give here an overview of the mechanisms and motivations leading players to get to know and to interact with each other. For more details see ref. 1.

Every game action carried out by a player (trade, movement, attack, etc.) costs a certain amount of so-called action points (APs). These points can not exceed a maximum value. For players having less APs than the maximum, every few minutes a small number of APs is replenished automatically. Once a player's character is out of APs, she has to wait to be able to play on. As a result, the typical Pardus player logs in once a day to spend all her APs on several activities within a few minutes. Social activities such as writing PMs do not consume APs.

A Pardus universe has the shape of a two-dimensional lattice (bounded in several ways) on which players can move (movement consumes action points). On each field (the smallest unit of this lattice), a player has the option to construct a building. Buildings act both as production sites and trade outlets for certain commodity types. Typically, a player has up to five buildings. Players may visit buildings of other players to trade game money for commodities or vice versa. A player has a trade tie with every other player who traded at her buildings, or whose buildings she traded with. Additionally, there is the (much rarer) possibility that two players meet on the same field and exchange game money and/or commodities. Attack comes with the same two options: Either a player attacks the building of another player or the player himself (for this interaction they again have to stand on the same field).

All other relations (communication, friendship, enmity, bounty) are independent of location in space, i.e., every player may write PMs to, mark as friend or enemy, or set a bounty on any other player at anytime, provided she knows the target's character name. This name is visible on the navigation screen when players stand on the same field, in an online list which shows all currently online players, in chat channels, and in the game's forums provided a player has posted a message in the corresponding place, as well as in several sections of the game such as on news pages. We suspect that the type of acquaintances a player makes during the course of the game depends strongly on her involvement in social activities. If the player does not show the preference of using provided ways of communication (PMs, chats, forums), her partners of friendship/enmity/bounty interaction are likely to show a high causal dependency with her visited locations in the game universe. On the other hand, a frequent use of communication tools may reduce this dependency, because then interactions take place with players independent of location.

Besides character names and online status being displayed on every player's personal PM contacts page for quick access, the friends and enemies lists serve game-mechanic purposes: Friends/enemies are automatically or optionally included/excluded for certain actions. For example, enemies of building owners are not able to use the services offered in the respective places. Note that friend and enemy markings need not necessarily denote *affective* friendships or enmity, they rather indicate a certain degree of cooperative or noncooperative stance motivated by affective and/or cognitive incentives. However, we assume these two motives to coincide to a considerable extent, e.g., it seems highly unlikely that someone marked as enemy/friend due to rational considerations at the same time constitutes the affective opposite of friend/enemy within the game (and vice versa).

We have no information about external forms of relation or communication, e.g., players being real-life friends or communicating via external tools. Further, so far we do not know how well structure and dynamics of different types of social networks in Pardus match comparable social networks in real life, with a few exceptions (1): We have shown good agreement of PM network features with properties of mobile phone call networks and revealed findings well according with classic sociological hypotheses. Further, we have begun studying positive and negative networks as single entities and found results highly consistent with social balance theory, as well as a coincidence of network properties (triad significance profiles) with nonvirtual social networks.

Comparison with Existing Datasets. To our knowledge, the only large-scale dataset incorporating multiple interactions is the Facebook network of Lewis et al. (2). Pardus offers several advantages over this Facebook data. The Facebook network consists of three types of interactions between users: declared friendship relationships, picture friendships (being tagged in an online photo by a user), and dorm roommate friendships. However, two of these three types of interactions lead to a tainted representation of the social system. First, the friendship network of Facebook is known to be biased by the visibility of the friends of a user on its webpage (6). In Pardus, friend and enemy lists are *completely private*, meaning that no one except the marking and marked players have information about positive or negative ties between them. Our data thus represents a more realistic social situation, in the sense that social ties are not immediately accessible to the public but need to be found out by communication with or by careful observation of others. Second, dorm membership is obtained from the projection of a bipartite network. This procedure is known to distort the number of cliques in a network (3). For this reason, we only focus on one-to-one interactions between players and discard indirect interactions such as the participation to a chat. Finally, the Pardus dataset has the advantage to capture a broad range of social interactions, because the players are immersed in the game and therefore not only communicate with one another, but also engage in collaborative/antagonistic actions.

Mathematical notations—Overlap. The standard way to represent a network is through its adjacency matrix A_{ij} which, for an unweighted, undirected network, is a symmetric matrix whose elements A_{ij} are equal to one if there is a link between i and j, and zero otherwise. To incorporate the existence of multiple relations (multiplex networks), it is common to define the tensor $A_{ij;\alpha}$, sometimes called supersociomatrix (4). This tensor has dimension $N \times N \times R$, where N is the total number of nodes and R is the number of different link types between the same set of agents. For a fixed value of α, $A_{ij;\alpha}$ is the adjacency matrix of the network defined by link type α. By construction, the properties of each network can be obtained from its adjacency matrix $A_{ij;\alpha}$. For instance, the degree $k_{i;\alpha}$ of a node i is given by $\sum_j A_{ij;\alpha}$, the total number of links in network α is $L_\alpha = \sum_i k_{i,\alpha}/2$. The number of paths of length n between nodes i and j is given by $(A_\alpha^n)_{ij}$. A whole new layer of complexity opens once the interplay between different sorts of networks is considered. From a mathematical point of view, multiplexity can be revealed by coupling different adjacency matrices. For instance, the (link) overlap $O_{\alpha\beta} = \frac{1}{2}\sum_{ij} A_{ij;\alpha} A_{ij;\beta}$ between the graphs α and β counts the number of links they have in common. Similarly, the multiplicity $m_{ij} = \sum_\alpha A_{ij;\alpha}$ of a link between i and j counts the number of different links between these nodes.

Correlation measures. Several network measures are based on the Pearson's correlation between two quantities. For two random variables X and Y with mean values $\bar{X}$ and $\bar{Y}$, and standard deviations σ_X and σ_Y, the correlation coefficient $\rho(X,Y)$ is defined as:

$$\rho(X,Y) = \frac{E[(X-\bar{X})(Y-\bar{Y})]}{\sigma_X \sigma_Y} \in [-1,1]. \qquad \textbf{[S1]}$$

The *reciprocity* coefficient r is the correlation coefficient between the transposed entries of the adjacency matrix of a directed graph, $X \equiv A_{ij}$, $Y \equiv A_{ji}$ (5). Similarly, we introduce the coefficients $\rho(k_\alpha^{\text{in}},k_\alpha^{\text{out}})$ to evaluate the correlations between in-degree and out-degree around the same node in a graph α and $\rho(k_\alpha,k_\beta)$, to evaluate the correlations between the degrees of a node in the two different graphs α and β. The coefficient $\rho(k_\alpha^{\text{in}},k_\alpha^{\text{out}})$ is a measure of the deviation of a directed network from a Eulerian network, i.e., $\rho(k_\alpha^{\text{in}},k_\alpha^{\text{out}}) = 1$ only for a Eulerian graph, namely $k_{i;\alpha}^{\text{in}} = k_{i;\alpha}^{\text{out}}$ for each node i, while $\rho(k_\alpha,k_\beta)$ measures the correlation of the degree centrality of the same node in different networks. The coefficient $\rho(\text{rk}(k_\alpha),\text{rk}(k_\beta))$ is calculated the same way as $\rho(k_\alpha,k_\beta)$, with the difference that not degrees but ranks of degrees are used, i.e., the node with largest degree has rank 1, the second largest has rank 2, etc. Nodes with the same degree have the same rank; the difference to the subsequent rank is the number of nodes which shared the previous rank. For example if there are three nodes with degree 45 and rank 10, nodes with degree 44 have rank 13.

Relations between network–network measures. Correlating network-network measures reveals a strong relation between link overlap and degree correlation ($\rho = 0.88$, p-value: 10^{-5}), see SI Fig. 1 (*a*). Pairs of networks of the same connotation have a higher overlap than oppositely connotated pairs; a similar tendency for degree correlation is apparent. A correlation between link overlap and degree rank correlation is also present, however with lower significance ($\rho = 0.63$, p-value: 0.01), see SI Fig. 1 (*b*). We mark pairs including a communication network as neutral, since messages may involve both positively or negatively connotated content.

Network-network interactions over time. To assess to what extent network-network properties of link overlap, degree correlation, and degree rank correlation change over time, we show these properties at days 150, 300, and 445 for all pairs of networks in SI Fig. 2. Here, accumulated networks, i.e., all except friendship and enmity networks, are accumulated over days 1 to 150, over days 1 to 300, and over days 1 to 445, respectively. Friendship and enmity networks are taken at these times. The number of players involved in the envelope network (i.e., in any relation) changes from 9,862 to 15,103 to 18,819 in these points in time, respectively. Changes are relatively small, except for degree correlations of pairs including bounty networks. Overlap values generally tend to decrease slightly over time.

Social balance and sparse networks. To analyze the multiplexity of large-scale networks and to draw conclusions from our observations, we need to address an issue that is usually obsolete for experiments on small social systems. When considering different types of interactions between students of a class or diplomatic positions between countries, it is reasonable to assume that all agents in the network are aware of each other's existence. In large-scale social networks, in contrast, the absence of any type of link between two nodes may either correspond to the existence of an indifferent/neutral interaction, or to the absence of any past and present contact between both agents. The fact that agents only know a fraction of the total set of agents is typical of sparse networks and originates from the finite capacities of its nodes, i.e., agents have limited time and resources, therefore can explore a small fraction of the available spatial and cognitive space. In the Pardus networks this finiteness is affirmed by the observation that out-degrees of friendship and enmity networks have an upper bound, limited by the Dunbar number of ≈150 (1), presumed as a natural limit for social ties humans are able to sustain (7). The average degree $\bar{k}_\alpha$ is well below $O(100)$, for all types α.

A proper null model. The aspect of a null model becomes important when assessing the relevance of topological structures in a network. A standard procedure consists in comparing this observation against similar observations in null models, i.e., randomized versions of the original network under adequate constraints (8). In order to test predictions of structural balance theory, we focus on friendship and enmity relations, and leave aside other types of interactions. In a first step, we remove the negligible number of ambiguous links (links between players where one marks the other as friend but is marked back as enemy). Our strategy is now to compare the numbers N_{Δ_i} of triads with i positive links with the expected numbers $N_{\Delta_i}^{\text{rand}}$ of triads in a null model. A standard choice for a null model consists of random graphs with fixed degree sequences. It has been applied for each network separately in Table 1, where we observe that friendship and enmity networks are both more transitive than a random graph. However, this choice is not appropriate to test the arrangement of positive and negative links on the set of existing relations between agents—a reshuffling of topology by keeping degrees fixed would for example considerably change the number of triads which we want to keep fixed. For this reason we define a null model by keeping the topology fixed and by randomly assigning the L_+ plus-signs and L_- minus-signs on the existing links, where L_+ (L_-) are the original numbers of friendship (enmity) links respectively. N_Δ^{rand} is measured by averaging over 1000 realizations of the null model. Moreover, the deviation of the data from randomness is evaluated by the so-called z-score:

$$z_i = \frac{N_{\Delta_i} - N_{\Delta_i}^{\mathrm{rand}}}{\sigma_{\Delta_i}}, \quad [2]$$

where σ_{Δ_i} is the standard deviation of the number of triads Δ_i.

Given the ratio $p := \frac{L_+}{L_+ + L_-}$ of positive to all links in a signed network, the expected ratio of triad types in the sign-shuffled null model is, following straightforward combinatorial arguments, p^3, $3(1-p)p^2$, $3(1-p)^2p$, and $(1-p)^3$ for triad types $+++$, $++-$, $+--$, $---$, respectively. These expressions were used to create Fig. 5 (center) in the main text.

Dynamics of signed triadic structures and network growth. By measuring all day-to-day transitions from wedges (triads with two links, with the possible forms $++$, $+-$, and $--$) to the other triadic structures ($+++$, $++-$, $+--$, $---$, $++$, $+-$, $--$, $+$, $-$, and the empty triad) we shed light upon the mechanisms which lead to the observed significant social balance discussed in the main text. We measure the following possible transition types: A wedge stays the same, closes with a positive/negative link (with the original links unchanged), has one or both links removed, or has the sign of one or both links switched. SI Fig. 3 shows the daily transition probabilities, normalized by the total number of wedges of the corresponding type on that day. Due to lack of notability the transition type of switching links (with a probability less than a tenth of that of link-removal, on average) was not included in SI Fig. 3.

Wedges of type $++$ close preferentially with a positive link, see green line in SI Fig. 3 (*a*), wedges of type $+-$ with a negative link, see blue line in SI Fig. 3 (*b*). These probabilities are decreasing over time and seem to eventually level out. There is no clear sign preference in the closure of type $--$ wedges (red lines). These observations consistently explain the social balance results shown in Fig. 4 and Fig. 5 in the main text. Further, note that $--$ wedges are much more likely to remain unchanged than other types of wedges, see SI Fig. 3 (*d*). We conclude that the mechanism of triadic closure (9) has a much weaker influence as a driving force in purely negative tie networks than in positive tie or signed networks.

SI Fig. 4 depicts the total number of wedges of each type, for every day. Note how the majority of wedges is of type $--$, although there are more positive than negative links, see Table 1 (main text). Also the growth rate for $--$ wedges is higher than for the other two types (until about day 350, where the number of $--$ wedges starts to equilibrate). This seemingly paradoxical circumstance is consistent with the marked differences in clustering coefficients, see Table 1 (main text). It is further consistent with the observation that a number of aggressive players frequently offend many others and consequently get marked as enemy by unconnected players (1). Since the clustering coefficient measures the 'closedness' of triads, a high clustering coefficient in friendship networks implies a relatively small number of $++$ wedges, whereas a low clustering coefficient in enmity networks implies a relatively high number of $--$ wedges.

For assessing to what extent network growth is driven by the closure of triads, we define the *closure ratio* as the number of newly added links which close at least one wedge, divided by the number of all new links, over a certain time-window during the evolution of the network. The closure ratio lies between 0 and 1; the higher it is the more new links close a wedge. In practice, the closure ratio is strictly smaller than 1, since a number of cases unavoidably do not allow for the possibility of new links closing a wedge (for example the first and second links which are added into an empty network because no wedges exist at that stage). The measured time-evolution of daily closure ratios in the friend-enmity multiplex-network is depicted in SI Fig. 5 (*a*). Over time the ratio slightly increases and seems to level out at around 0.5 for both positive and negative links. We conclude that half of all links added close at least one wedge, while the other half does not close one. Thus, a model for network growth using only wedge transition rates shown in SI Fig. 3 could only account for the dynamics of about half of the added links.

Another quantity important for modeling social network dynamics is the number of removed links per time. We define the *link churn* ch as the number of removed links divided by the number of new links, over a given time-window. The churn is nonnegative; there are 3 possible cases: *i*) Growth ($0 \le \mathrm{ch} < 1$): More new than removed links, *ii*) Equilibrium ($\mathrm{ch} = 1$): The same number of new as removed links, *iii*) Shrinkage ($\mathrm{ch} > 1$): More removed than new links. The higher ch, the more links are removed relative to the number of added links. Note that in the majority of classic network growth models, such as preferential attachment (10), no removal of links is assumed ($\mathrm{ch} = 0$) and the effect of churn is ignored. The measured time-evolution of link churns over time windows of 14 days in the friend/enmity network is depicted in SI Fig. 5 (*b*). Over time ch increases and fluctuates around $\mathrm{ch} = 0.7$ for both positive and negative links (taken over days 200 to 445, $\mathrm{ch} = 0.66$ for friend links and $\mathrm{ch} = 0.72$ for enemy links). Therefore, at the end for every three new links about two links are removed. Since the number of links removed from wedges is much smaller than links added to close wedges, we conclude that many links are removed from triadic structures other than wedges. Again, a model for network growth using only the transition rates shown in SI Fig. 3 would only account partially for link-removal dynamics.

A network evolution model of signed triadic closure. Using the measured daily transition rates above we define a transition matrix

$$M_{\mathrm{STC}} = P\begin{pmatrix} ++ \to +++ & ++ \to ++- & ++ \to ++ \\ +- \to +-+ & +- \to +-- & +- \to +- \\ -- \to --+ & -- \to --- & -- \to -- \end{pmatrix} = \begin{pmatrix} 0.000212 & 0.000029 & 0.999759 \\ 0.000025 & 0.000279 & 0.999696 \\ 0.000040 & 0.000036 & 0.999924 \end{pmatrix},$$

where the entries are the probabilities of a wedge of given type to another triadic structure. Rows 1, 2, and 3 of M_{STC} distinguish between wedge types $++$, $+-$, and $--$, respectively; columns 1, 2 and 3 distinguish between probabilities for closure with either a positive or a negative link, or the probability of no change, respectively. The constant probabilities of columns 1 and 2 are determined by averaging the corresponding evolving probabilities over the days 100 to 445 (this time-window was chosen due to a relatively decreased level of fluctuations in transition probabilities, see SI Fig. 3). The third column is one minus the sum of values in column 1 and 2, since we neglect link-removals and sign-switches. With these parameters we design the following network evolution model, to understand *Signed Triadic Closure (STC)*:

- At time t pick wedge i at random (random sequential update)
- Determine the type of wedge i and close (or do not close) it according to the relevant entry in M_{STC}
- Pick next wedge until all wedges are updated
- Continue with time step $t+1$

As initial condition we take the observed friendship and enmity multiplex-network at day 100. Simulating this process leads to the results shown in Fig. 5 (right) in the main text, reproducing the ratio of triads in the data considerably better than the null model.

For the purpose of simplicity, the STC model ignores three possibly important aspects:

- It does not take into account links added by means other than triadic closure. As we have shown above, the closure ratio ≈ 0.5, i.e., only half of all new links are added in the process of triadic closure. For the other half of new links, one could for example take into account the mechanism of preferential attachment (10), for which exponents were reported in (1).

- The model does not take into account the removal of links. Because removal happens in a relatively high frequency ($ch \approx 0.7$), a possible extension of the model could involve the measurement and implementation of decay rates, i.e., of transition rates from complete signed triads to wedges (or other triadic structures with a smaller number of links). We suspect that balanced triads are more stable than unbalanced triads.
- The model could be expanded to incorporate directed links and in/out-degree distributions, clustering coefficients, assortativity, etc.

1. Szell M, Thurner S (2009) Measuring social dynamics in a massive multiplayer online game. arXiv:0911.1084.
2. Lewis K, Kaufman J, Gonzalez M, Wimmer A, Christakis N (2008) Tastes, ties, and time: a new social network dataset using facebook.com. *Social Networks* 30:330–342.
3. Newman MEJ, Strogatz SH, Watts DJ (2001) Random graphs with arbitrary degree distributions and their applications. *Phys Rev E* 64:026118.
4. Wasserman S, Faust K (1994) Social network analysis: methods and applications (Cambridge University Press).
5. Garlaschelli D, Loffredo MI (2004) Patterns of link reciprocity in directed networks. *Phys Rev Lett* 93:268701.
6. Golder S, Wilkinson D, Huberman B (2007) Rhythms of social interaction: Messaging within a massive online network. In Communities and Technologies 2007: Proceedings of the Third Communities and Technologies Conference (Springer, New York).
7. Dunbar R (1993) Co-evolution of neocortex size, group size and language in humans. *Behavioral and Brain Sciences* 16:681–735.
8. Maslov S, Sneppen K (2002) Specificity and stability in topology of protein networks. *Science* 296:910–913.
9. Rapoport A (1953) Spread of information through a population with socio-structural bias I: assumption of transitivity. *Bull Math Biophys* 15:523–533.
10. Barabási A, Albert R (1999) Emergence of scaling in random networks. *Science* 286:5439 509.

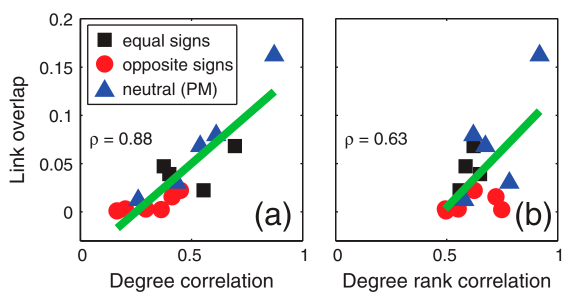

Fig. S1. Correlation between the network-network measures of (*a*) link overlap and degree correlation (*p*-value: 10^{-5}), (*b*) link overlap and degree rank correlation (*p*-value: 0.01). Pairs of networks with equal connotation (positive-positive or negative-negative) have a higher overlap then oppositely signed pairs, with a similar tendency for degree correlation. We mark pairs including a communication network as neutral, since messages may involve both positively or negatively connotated content.

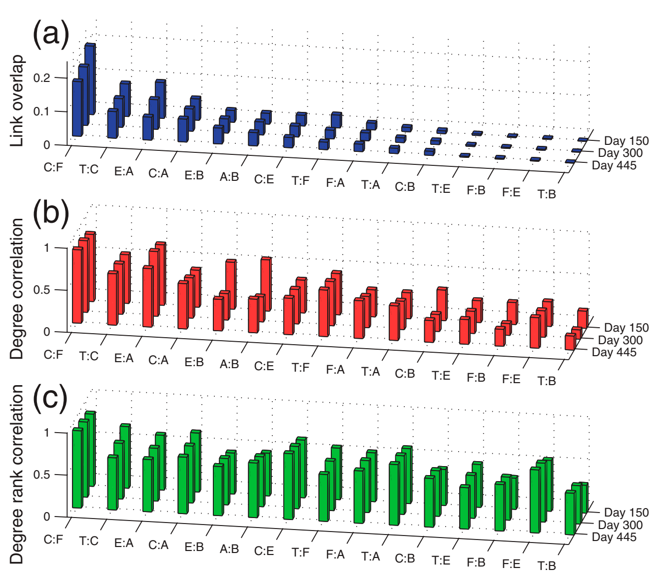

Fig. S2. Evolving network-network properties (*a*) link overlap, (*b*) degree correlation, (*c*) degree rank correlation, on the days 150, 300, and 445, for all pairs of networks, with the notations E for Enmity, F for Friendship, A for Attack, T for Trade, C for Communication and B for Bounty. Changes are relatively small, except for degree correlations in the E:B, A:B, C:B, and F:B interactions.

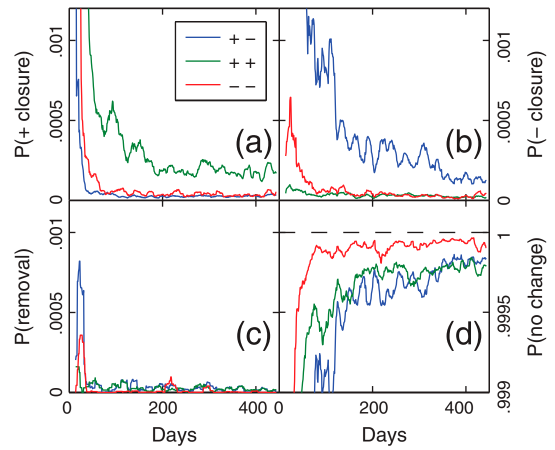

Fig. S3. Measured day-to-day transition probabilities from wedges to staying the same or to other triadic structures, in the multiplex-network consisting of friend and enmity relations. For visual clarity a moving average filter with a time-window of 14 days was applied. (*a*) Probabilities of wedges being closed with a positive link. (*b*) Probability of a wedge being closed with a negative link. (*c*) Probability of a wedge having one or both links removed. (*d*) Probability of a wedge staying unchanged. Note how + + wedges have a clear preference of being closed by a positive link, while + − wedges have a clear preference of being closed by a negative link. Wedges of type − − have no sign preference for closure and are more likely to remain unchanged than other wedge types.

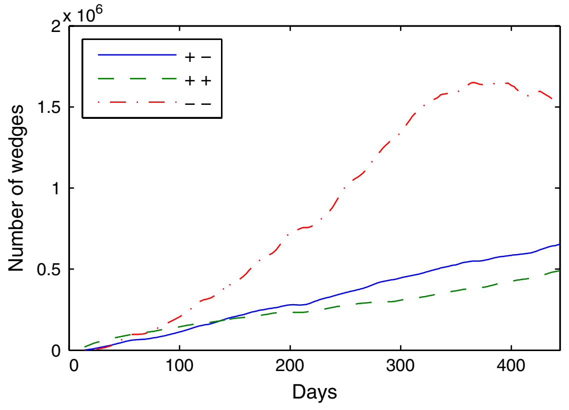

Fig. S4. Evolution of number of wedges of each type, in the multiplex network consisting of friend and enmity relations. For visual clarity a moving average filter with a time window of 14 days was applied.

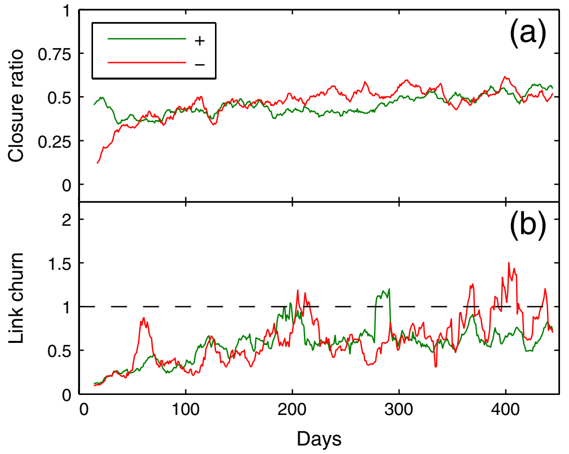

Fig. S5. (*a*) Closure ratio, defined as the number of new links which closed at least one wedge divided by all new links, here for each day. For visual clarity a moving average filter with a time window of 14 days was applied. (*b*) Link churn ch, defined as the number of links removed divided by the number of links added, here for each time window of 14 days. Evolutions of these ratios are depicted for positive and negative links, within the multiplex network consisting of friend and enmity relations.